

STUDY ON THE DYNAMIC RESPONSE OF DEEP-SEA TRAWLERS IN SEA TRIALS


Qingchao Xu  ¹

Yonghe Xie  ¹

Hao Cai  ¹

Xiwu Gong *  ¹

Detang Li ¹

Wei Wang  ^{2,3}

Panpan Jia  ⁴

¹ School of Naval Architecture and Maritime, Zhejiang Ocean University, Zhoushan, Zhejiang, China

² School of Naval Architecture Ocean and Civil Engineering, Shanghai Jiaotong University, Shanghai, China

³ Marine Design and Research Institute of China, Shanghai, China

⁴ School of Naval Architecture, Ocean and Energy Power Engineering, Wuhan University of Technology, Wuhan, Hubei, China

* Corresponding author: gongwinfish@126.com (Xiwu Gong)

ABSTRACT

The increasing use of automation in fishing vessels has improved trawling efficiency while directly affecting the fishing capacity and cost of fishing vessels. Among the various influencing factors, warp tension and warp length can be varied to automatically balance the retraction and release of warp control. We combined the two parameters and independently designed and developed the key equipment for fishing vessels—the warp dynamometer and meter counter—and control software. The accuracy of the warp tension and length measurements was improved. The designed equipment was applied to sea trials under different working conditions, and the test data records were exported. Next, filtered time-domain graphs of the required parameters were plotted through complex Fourier transform, first-order low-pass filtering, and inverse Fourier transform. The results of data processing using various parameters were compared and analysed to determine the variation trends of the parameters and verify the effects of their balance control. The results indicated that using an automatic balance control system that combines warp tension and warp length can be effective for the fishing operation of offshore double-deck trawlers. In addition, first-order low-pass filtering can be used to filter complex warp tension data. This study also determined the relationship between warp tension and experimental parameters such as warp length and ship speed during the release of control. After the balance control of warp tension and warp length, the net mouth area increased by 30.7% and 36.5%, respectively, and the fishing efficiency of the vessel improved considerably.

Keywords: Trawler; Automation; Warp tension; Warp length; Ship speed

INTRODUCTION

Trawling is a primary method used in fishing operations. In this method, warps are used to connect the trawler to an end fishing net, which is dragged in the water to capture fish. The net is placed in the water layer by retracting and releasing the warps and by adjusting the ship speed. Towed fishing equipment primarily includes trawler winches, trawlers, and netting (otter board, trawler net, net bag, etc.). The degree of automation in existing fishing trawlers is low, and crew

members are unaware of the working principles of warp retraction and release in fishing systems. The knowledge of fishing operations is mostly experiential and not based on a scientific rationale. If warp retraction is excessively delayed, excessive amounts of fish are caught in the net, thereby increasing the pressure on the net. By contrast, if the warp is prematurely retracted, excessively few fish are caught, thereby decreasing the fishing efficiency and resulting in failure to achieve the fishing target. Furthermore, if the net is trawled to the seabed, the net may break.

Researchers worldwide have attempted to develop excellent trawling systems to address the aforementioned problems. Cho et al. [1] performed field experiments in the sea near Kokunsan Is. in the Western Korean Sea and summarized the variation trends of parameters such as warp length and towing speed. Hu et al. [2] designed a trawl depth controller based on the actual motion of mid-level trawls. Johansen et al. [3] proposed the use of horizontal motion in trawl systems. Cha and Lee [4] performed dynamic simulations of a midwater trawling system. Reite et al. [5, 6] installed a brake on a net plate to control the trawling depth and performed sea trials to verify the effectiveness of the system. Zand [7] realized stability control through a composite control strategy using a tugboat and a towing winch. Lee et al. [8] designed and simulated the dynamic motion of a novel fishing gear system. Sun [9] and Chen [10] designed trawling systems and developed corresponding models. Balash et al. [11] developed a novel prawn trawler design to reduce drag in trawling systems. Carral et al. [12] proposed a relationship between fishing winch design parameters and the operating depth of fishing gear. Su et al. [13] focused on the warp length of a trawling system. Juza et al. [14] introduced a two-boat setup for continuous trawling for quicker and more convenient trawling, even in deep water layers; this setup helps achieve more accurate distance and depth measurements. Park and Lee [15] adjusted the trawler direction and warp length during trawling for the automatic control of the trawler gear depth.

Most existing warp control systems in trawlers are based on either warp tension balance control or warp length (depth) balance control. Few studies have combined both parameters (warp tension and warp length) to achieve balance control. In the present study, with an ocean-going double-deck trawler as a reference, both warp tension and length were utilized to determine the warp parameters and achieve their automatic balance control. The key components and the corresponding control software used for measuring the tension and length of the warp were designed and fabricated independently, and breakthrough measurement accuracy was achieved. By analysing the warp parameters obtained from the test, the superiority of the automatic trawling balance control system is verified. Combined with the analysis of warp parameters and net mouth parameters, the final outstanding results can be summarized as follows: the net mouth area increased by 30.7% and 36.5% after the balance control of the warp tension and warp length, respectively. This was superior to the previously achieved 9.6% increase in the net mouth area through only warp tension balance control, thereby improving the fishing efficiency of the trawler.

SEA TRIAL

EXPERIMENTAL PREPARATION: TWO IMPORTANT DEVICES

Warp dynamometer

The warp dynamometer is an instrument used for measuring warp tension during the dragging of a trawling net. To evaluate

warp tension, pressure P was first measured using a pressure sensor installed on a pulley shaft. Eq. (1) was used to calculate the tension T on the wire rope around the pulley. The warp tension was synchronously calculated and recorded using our self-developed warp automatic control software.

$$T = P/2\sin\theta \quad (1)$$

where T denotes warp tension, N; the unit used in the experiment was kg (0–3000 kg). Warp tension refers to mutual traction in the interior of a warp and is perpendicular to the contact surfaces of the two adjacent parts when the warp is subjected to a pulling force. P in Eq. (1) denotes the load on the central roller, N; θ is the angle between the rollers and was set to 30° in this experiment. Fig. 1 displays a SolidWorks 3D model of the warp dynamometer and the installation rendering. The yellow part of the equipment displayed in Fig. 1(b) is a retracting and releasing warp device called a trawler winch, which can be used for balance control.

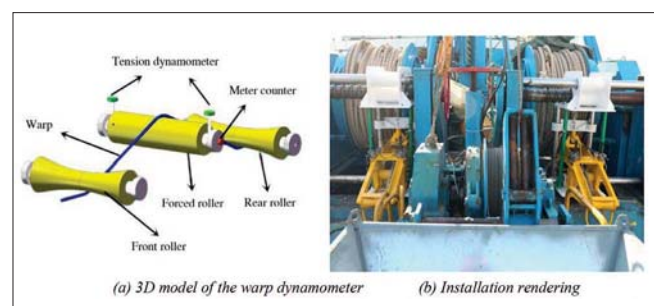


Fig.1. 3D model and installation renderings of the warp dynamometer

A DLS–electronic boom was used to calibrate the warp dynamometer. The calibration results of the warp dynamometer are listed in Table 1.

Tab. 1. Calibration results of the warp dynamometer

Electronic boom (kg)	367.0	497.0	588.0	730.0	960.0	1007.0
Warp dynamometer (kg)	367.5	497.2	588.7	729.3	959.1	1007.5
Error (%)	0.13	0.04	0.12	0.10	0.09	0.05

The values for the electronic boom and the warp dynamometer displayed in Table 1 were compared; the error between the two was extremely small ($<0.15\%$) and satisfied the accuracy requirements.

Meter counter

The meter counter is a device used for measuring length and can be used in all equipment designed for length measurement and control. Meter counters were used to accurately measure the warp length in this study. The meter counters were installed on the forced roller axis of the left and right warp dynamometers to calibrate the length measurement of the warp dynamometer. The SolidWorks 3D model of the meter counter is displayed in Fig. 2(a). This device is depicted in Fig. 2(b) as the black sensor at the end of the wire and the entire parallel part of the middle roller.

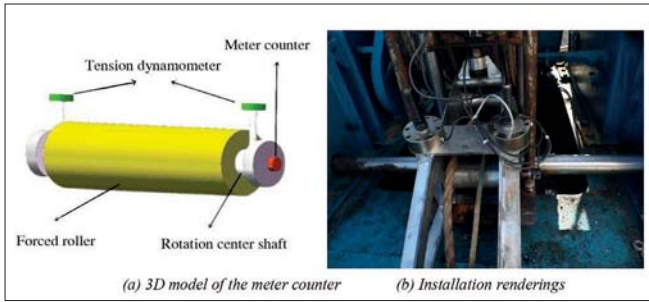


Fig. 2. 3D model and installation renderings of the meter counter

The meter counter required debugging and calibration. To improve the accuracy of the meter counter, every 10 m from one end of the warp was marked with paint; 10 m was marked with red paint, 20 m was marked with yellow paint, and so on until the mark reached 60 m. The calibration results of the warp length meter are presented in Table 2.

Tab. 2. Calibration results of the warp length meter

Measured warp length (m)	10.00	20.00	30.00	40.00	50.00
Warp length meter (m)	9.89	19.90	29.90	39.89	49.88
Error (%)	1.10	0.50	0.33	0.28	0.24

As displayed in Table 2, the error of the warp length meter was less than 1.5%, and the measurement accuracy was higher than that of existing warp length meters.

TRAWLING CONTROL

Automatic trawling control, in fact, is mainly achieved by the automatic retraction and release of the warp. The automatic warp winch control system was then independently designed by us.

The working principle of the automatic warp winch control system is as follows: The parameter data of the warp (e.g., warp tension and warp length) are acquired in real time during the retraction, release and dragging of the warp. The data are then transmitted to a self-designed warp automatic control software in the form of electrical signals. The parameter control conditions are set in advance, and the control instructions are judged and fed back to the hydraulic press to realize the automatic control of the warp winch. The self-designed control software interface of the warp winch is displayed in Fig. 3.



Fig. 3. The control software interface of the warp winch

EXPERIMENTAL PROCESS

In the first experiment, we performed calibration in the vicinity of 16 NM to the southeast of Zhujiajian, Zhoushan, China, where the water depth was 30 m.

In the second experiment, we sailed 27 NM in the direction of Zhujiajian, Zhoushan, China and reached Dongfushan, where the water depth was 50–65 m. After calibration, we performed experiments for automatic trawling control and net shape monitoring and control.

In the third experiment, we sailed 10 NM from the east of Zhujiajian, Zhoushan, China to the east of Andao in the outer ocean and reached a water depth of 30–35 m and performed a complete acceptance test by integrating fully automated intelligent fishing, fish transfer, refrigeration, and preservation. Furthermore, we analysed the roundabout motion of the ship and recorded the relevant data. Fig. 4 displays the images used in the third real sea test.



Fig. 4. Scene of the third real sea test

Vettor [16] developed a new scheme to better estimate ship performance and response to sea conditions. Gucma [17] defined the relationship between port waterway system elements and conditions for the safe operation of ships. The experimental parameter setting values were obtained during the sea trial under actual sea conditions, as displayed in Table 3.

Tab. 3. Field test conditions

Designated water depth (m)	Length of the releasing warp (m)	Ship speed (kn)
20	80-100-105-110-130	2.5-3.0-3.5-4.0-4.5
50	80-100-105-110-130	2.5-3.0-3.5-4.0-4.5
30	80-100-105-110-130	2.5-3.0-3.5-4.0-4.5

AIS DATA

After the experiment, the sea state navigation chart from 2021-12-03 to 2021-12-04 (Fig. 5) obtained from the ship information network was analysed.

The AIS data are displayed in Fig. 5: the angle in the heading direction was 293.0°, the angle in the track direction was 270.0°,

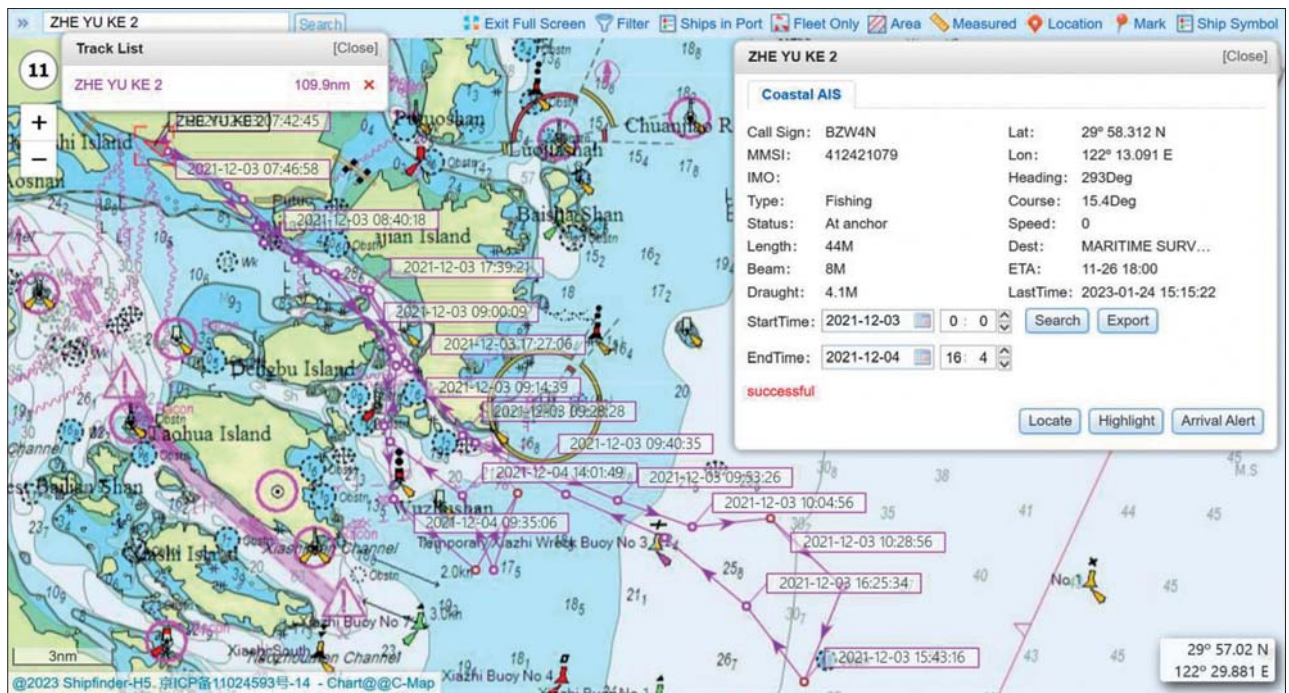


Fig. 5. Navigation chart of sea conditions

the latitude was 29° - 58.312° N, and the longitude was 122° - 13.091° E.

EXPERIMENTAL DATA PROCESSING

TIME-DOMAIN GRAPHS

MATLAB software was used to process the data in the Excel file to obtain time-domain graphs. Fig. 6 displays the time-domain graph of the warp length in the sea trial from 10:14 to 12:15 on 2021-12-04.

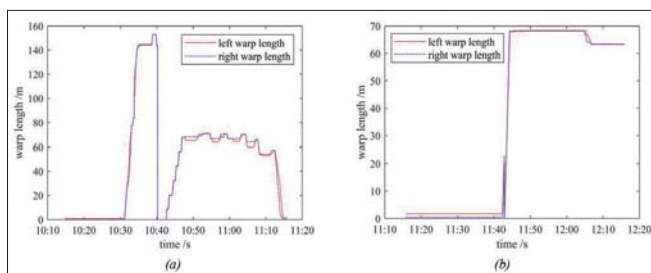


Fig. 6. Time-domain graph of the warp length

Fig. 7 displays the time-domain graph of the warp force in the sea trial from 10:14 to 12:15 on 2021-12-04.

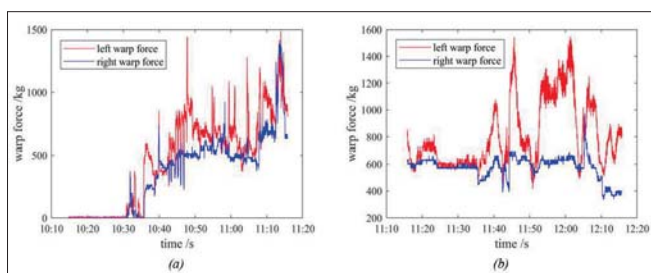


Fig. 7. Time-domain graph of warp force

The time-domain graph of the warp force indicated that the changes in data of the warp force were considerably unstable, with frequent large fluctuations; thus, filtering is necessary. Wang [18] analysed the factors affecting warp tension measurement and concluded that time-varying filtering and the variations in first-order low-pass filtering data are complex and challenging and that Kalman filtering requirements were not satisfied. Therefore, a digital filtering algorithm was proposed to filter out the signals that cause interference. The previous study [18] designed a digital filter that was an improvement over an amplitude-limited filter. In the present study, the designed first-order low-pass filter was an improvement over a frequency-limited filter. In this paper, interfering signals were effectively filtered through complex first-order low-pass filtering.

Interference was filtered through frequency-domain filtering, which roughly involved three steps, as illustrated in Fig. 8.

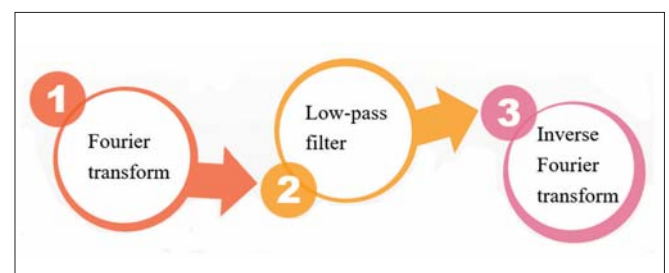


Fig. 8. Frequency-domain filtering process

FOURIER TRANSFORM

Fourier transform is a key algorithm in the field of digital signal processing. Vinay and John [19] authored a book titled Digital Signal Processing Using MATLAB (Third Edition), which covers topics such as discrete Fourier transforms and filter implementations.

Fig. 9 illustrates the steps involved in the Fast Fourier Transform (FFT) operation performed in this study.

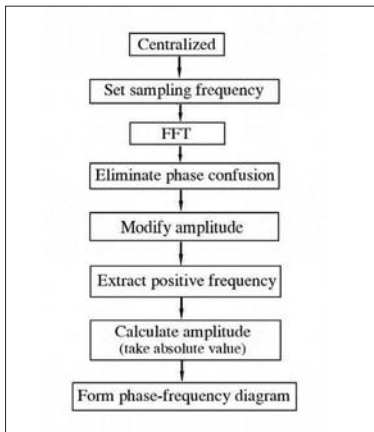


Fig. 9. FFT process in MATLAB

LOW-PASS FILTERING

The low-pass filter was set to a cutoff frequency. The simplest and most commonly used method to determine the cutoff frequency in the order of high to low involves using a low-pass filter and observing the filtering effect until ideal filtering is achieved. The part above the cutoff frequency is set to zero, and the part below the cutoff frequency retains its value. In this study, we employed different cutoff frequencies, observed the effects of filtering, and finally set the cutoff frequency as 150 Hz.

INVERSE FOURIER TRANSFORM

Because the frequency-domain graph of the Fourier transform is axisymmetric, the left half of the frequency domain graph is typically discarded for more effective analysis and physical representation. Therefore, to obtain a complete inverse Fourier-transformed time-domain graph, the half spectrum was completed to form a full spectrum. The frequency-domain data was then converted to time-domain data using the Inverse Fast Fourier Transform (IFFT) algorithm (executed using MATLAB).

The time-domain graph of the warp force after filtering on 2021-12-04 is displayed in Fig. 10.

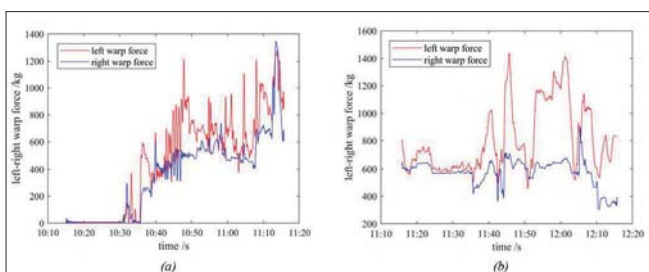


Fig. 10. Filtered time-domain graph of warp force

Using the same method of filtering for the ship speed, the time-domain graph of the ship speed was obtained after filtering on 2021-12-04 (Fig. 11).

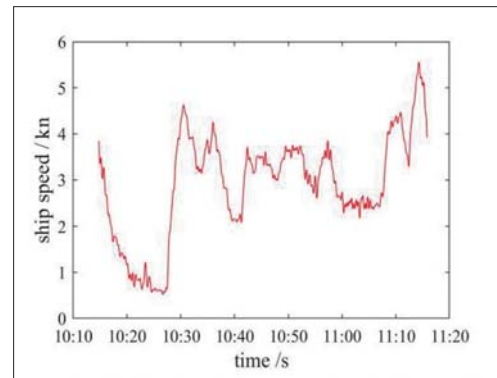


Fig. 11. Filtered time-domain graph of ship speed

The time-domain graphs obtained before and after filtering were analysed and compared:

1. The variation trends in the time-domain curves obtained before and after filtering were identical and almost coincident. Thus, our filtering operation was reasonable and satisfied the filtering requirements.
2. The filtered time-domain data of the warp force was mostly consistent with the time-domain data before filtering, with only a small degree of data reduction at extreme points. In the time-domain graph, the peaks corresponding to data changes at extreme points were not relatively sharp as expected, indicating that the filtering effect was favourable and eliminated the redundant signal interference.
3. The filtered time-domain graph was considerably clearer than the unfiltered time-domain graph because the frequency of the time-domain data obtained before filtering was 1 point/s (sampling frequency); the time-domain data points were denser, and the time domain curve was thicker with frequent fluctuations. The filtered time-domain graph did not exhibit these limitations and was thus better.

NUMERICAL ANALYSIS AND PROCESSING RESULTS

INFLUENCE OF EXPERIMENTAL PARAMETERS ON WARP FORCE

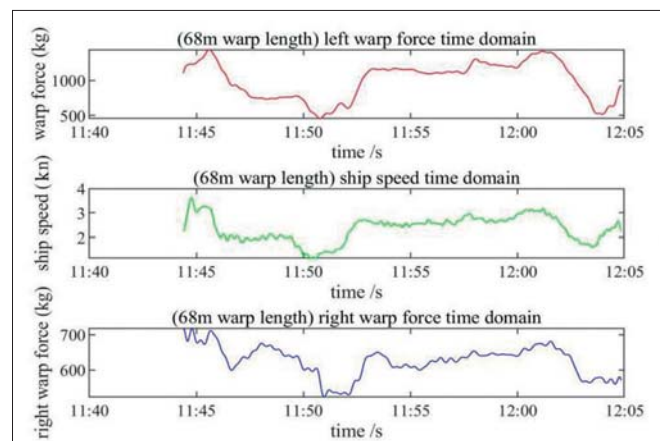


Fig. 12. Changes in warp force and ship speed in the time domain

With the warp length fixed at 68 m, the variation trends of the warp force and ship speed were observed. As displayed in Fig. 12, the time-domain curves of the left and right warp forces were similar to that of the ship speed time. Therefore, warp force was positively correlated with ship speed.

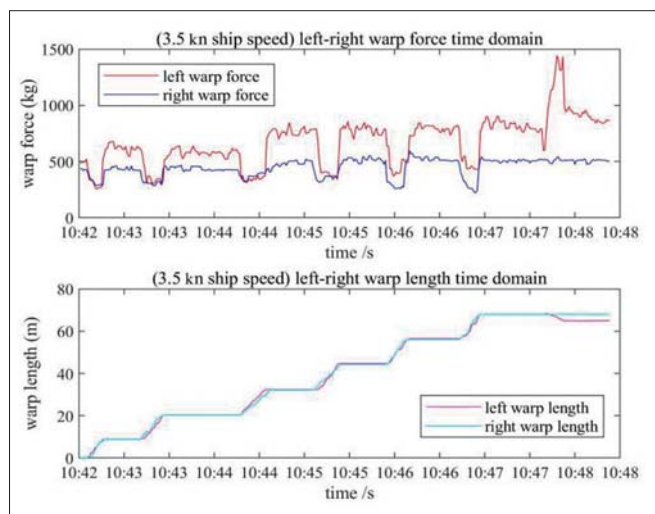


Fig. 13. Changes in warp force and warp length in the time domain

As illustrated in Fig. 13, the warp force and warp length were observed at a ship speed of 3.5 kn. The warp force decreased with increasing warp length because an increase in warp length occurred when the warp was released, thereby resulting in the relaxation of the warp and a decrease in warp tension. When the warp length was increased and stabilized, the warp tension increased rapidly. Moreover, the warp tension increased after stabilization compared to before. Thus, warp force was positively correlated to warp length.

ANALYSIS OF BALANCE ADJUSTMENT OF LEFT-RIGHT WARP

In this experiment, to verify the performance of the automatic balance adjustment of the left-right warp length, a test was performed to control the length difference between the left and right warps and realize balance adjustment. Table 4 displays the set working conditions and the test results.

Tab. 4. Automatic balance adjustment of the left-right warp length

Number of times	1	2	3	4	5	6
Difference before balance adjustment (left-right) (m)	-3	-2	-1	1	2	3
Difference after balance adjustment (left-right) (m)	0.2	0	-0.1	-0.2	-0.1	0
Time cost(s)	30	18	6	5	13	22

To verify the automatic balance adjustment of the left and right warp force, the results before and after the automatic balance adjustment were recorded (Table 5).

Tab. 5. Automatic balance adjustment of the left-right warp force

Number of times	1		2		3	
	Before	After	Before	After	Before	After
Left warp force (kg)	929.37	526.53	1096.73	1024.18	821.40	916.77
Right warp force (kg)	542.81	514.33	1356.95	1018.88	1125.80	919.42
Difference between left and right warp force (left-right) (kg)	386.56	12.20	-260.22	5.30	-304.40	-2.65

After balance adjustment, the lengths of the left and right warps and the warp force were balanced and stable.

VARIATIONS IN NET SHAPE OF THE BALANCE CONTROL SYSTEM

Wang et al. [20] designed a tension control system to effectively adjust net mouth expansion and improve fishing efficiency. Nsangue et al. [21] used a trawl model of the Antarctic krill fishery and tested it in a water tank; they investigated the effects of the flow velocity, horizontal spread ratio, sinking force, and the ratio of buoyancy to the fishing line weight. In [21], Eq. (2) was used to calculate the area of the net mouth (M_A).

$$M_A = \pi \times H \times CD/4 \quad (2)$$

where H denotes the net mouth height (vertical opening) and CD is the horizontal opening of the trawl net.

We determined the net shape parameters before and after the automatic balance adjustment of the warp that was realized using the net position meter system. Fig. 14 displays the net position monitoring interface of the net position monitoring and control system. This interface can not only be used to monitor the net position and net mouth information but also determine the required vertical expansion value of the net mouth.



Fig. 14. Monitoring interface of the net position

Fig. 15 displays the otter board monitoring interface of the net position monitoring and control system. This interface can be used not only to monitor the posture and information of the otter board but also to determine the horizontal expansion value of the net mouth.

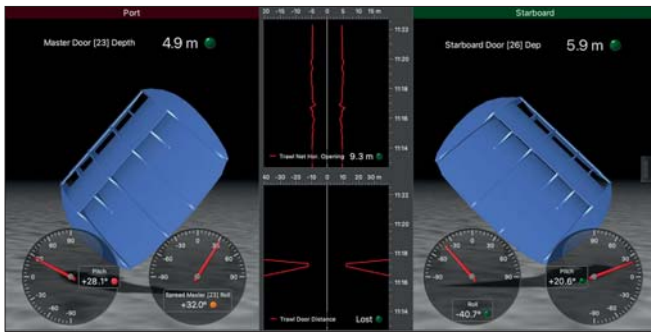


Fig. 15. Monitoring interface of the otter board

The horizontal expansion value of the net mouth was determined as follows: two net sleeve sensors were installed on both sides of the net mouth transverse position, and the distance between the two ends was the horizontal expansion value of the net mouth.

The vertical expansion value of the net mouth was determined as follows: the distance between the lower dragline and the upper dragline was measured using an upper dragline sensor based on the principle of acoustic echo.

Fig. 16 displays the time-domain graph of the horizontal expansion value of the net mouth obtained in the sea trial from 10:45 to 13:00 on 2021-12-04.

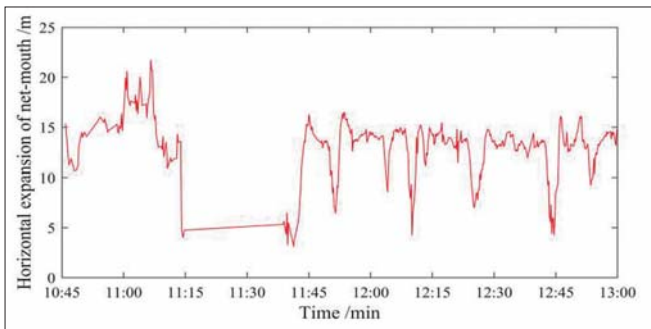


Fig. 16. Time-domain graph of the horizontal expansion value of the net mouth

Fig. 17 displays the time-domain graph of the vertical expansion value of the net mouth obtained in the sea trial from 10:45 to 13:00 on 2021-12-04.

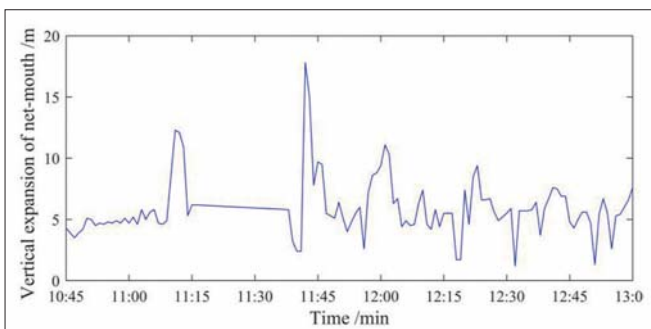


Fig. 17. Time-domain graph of the vertical expansion value of the net mouth

Furthermore, using Eq. (2) and the derived horizontal expansion and vertical expansion values of the net mouth, the net mouth area was calculated and then analysed. Table 6 displays the net shape data obtained when warp tension balance control was used.

Tab. 6. Net shape parameters under tension balance control

System	Horizontal expansion of net mouth (m)	Vertical expansion of net mouth (m)	Area of net mouth (m ²)
Without tension balance control	13.1	4.2	43.19
With tension balance control	15.3	4.7	56.45

Table 7 displays the corresponding net shape data obtained when warp length balance control was used.

Tab. 7. Net shape parameters under length balance control

System	Horizontal expansion of net mouth (m)	Vertical expansion of net mouth (m)	Area of net mouth (m ²)
Without length balance control	18.1	4.7	66.78
With length balance control	13.5	8.6	91.14

The net mouth area increased by 30.7% and 36.5% after balance control of the warp tension and warp length, respectively. By contrast, the net mouth area increased by 9.6% when tension control was used in a previous study [20]. Therefore, the present study further improved the fishing efficiency of the trawler.

CONCLUSIONS

The present study combined warp tension and warp length automatic balance control. In addition, key equipment was independently developed and designed, and sea trials were conducted through intelligent automatic fishing in ocean-going double-deck trawlers. The main conclusions of this study are as follows:

- (1) The innovative automatic balance control system that utilized both warp tension and warp length exhibited good performance and high accuracy, indicating the applicability of the proposed control system to fishing in ocean-going double-deck trawlers.
- (2) Warp tension was effectively evaluated through complex first-order low-pass filtering, with a filtering cutoff frequency of 150 Hz (when the data volume was 3600) for the parameter data in the warp balance system.
- (3) The warp force was positively correlated with warp length and ship speed.
- (4) The net mouth area increased by 30.7% and 36.5% after balance control of the warp tension and warp length, respectively, and the fishing efficiency thus improved.

In future studies, more experimental data related to straight navigation will be collected during sea trials; the data obtained during straight navigation and turns will be compared to derive the corresponding variation trends.

ACKNOWLEDGEMENTS

This study was financially supported by the “Pioneer” and “Leading Goose” R&D Program of Zhejiang (2022C03023), and Key R&D Projects in Zhejiang Province (2019C02087).

We thank all the reviewers who reviewed our manuscript. We also thank MJ Editor (www.mjeditor.com) for providing English editing services during the preparation of this manuscript.

REFERENCES

1. B. K. Cho and S. O. Cho, "A study on the bottom trawl gear by the trial of a stern trawler I - on the resistance of a bottom trawl gear," *Journal of Applied Mathematics and Informatics*, 2000.
2. F. X. Hu, T. Tokai and K. Matuda, "A computer simulation for the net position control of midwater trawl system," *Nippon Suisan Gakkaishi*, vol. 67, no. 2, pp. 226-230, 2001.
3. V. Johansen, O. Egeland and A. J. Sorensen, "Modelling and control of a trawl system in the transversal direction," *Control Applications in Marine Systems*, vol. 34, no. 7, pp. 243-248, 2002. [https://doi.org/10.1016/S1474-6670\(17\)35090-5](https://doi.org/10.1016/S1474-6670(17)35090-5)
4. B. Cha and C. Lee, "Dynamic simulation of a midwater trawl system's behaviour," *Fisheries Science*, vol. 68, no. 2, pp. 1865-1868, 2002. https://doi.org/10.2331/fishsci.68.sup2_1865
5. K. J. Reite and A. J. Sorensen, "Hydrodynamic properties important for control of trawl doors," *IFAC Conference on Control Applications in Marine System (CAMS 2004)*, vol. 37, no. 10, pp. 143-148, 2004. [https://doi.org/10.1016/S1474-6670\(17\)31722-6](https://doi.org/10.1016/S1474-6670(17)31722-6)
6. K. J. Reite, "Modeling and control of trawl systems," Norwegian University of Science and Technology, pp. 153-192, 2006.
7. J. D. M. Zand, B. J. Buckham and D. Constantinescu, "Ship and winch regulation for remotely operated vehicle's waypoint navigation," *International Journal of Offshore and Polar Engineering*, vol. 19, no. 3, pp. 214-223, 2009.
8. J. H. Lee, C. W. Lee and M. Y. Choe, "Applying fishing-gear simulation software to better estimate fished space as fishing effort," *Fisheries and Aquatic Sciences*, vol. 14, no. 2, pp. 138-147, 2011. <https://doi.org/10.5657/FAS.2011.0138>
9. X. F. Sun, *Modelling and simulation of single-vessel mid-level trawling system*. Dalian Maritime University, 2008.
10. Y. L. Chen, *Modeling and control of trawling towing system*. Zhejiang University, 2013.
11. C. Balash, D. Sterling, J. Binns, G. Thomas and N. Bose, "The effect of mesh orientation on netting drag and its application to innovative prawn trawl design," *Fisheries Research*, vol. 164, pp. 206-213, 2015. <https://doi.org/10.1016/j.fishres.2014.11.018>
12. J. Carral, L. Carral, M. Lamas and M. J. Rodriguez, "Fishing grounds' influence on trawler winch design," *Ocean Engineering*, vol. 102, pp. 136-145, 2015. <https://doi.org/10.1016/j.oceaneng.2015.04.055>
13. Z. P. Su, L. X. Xu, G. P. Zhu, Z. Wang, G. S. Hu and Y. J. Yu, "Effects of drag speed and warp length on the net position of mid-layer trawling of Antarctic krill," *China Fisheries Science*, vol. 24, no. 04, pp. 884-892, 2017. <https://doi.org/10.3724/SP.J.1118.2017.16229>
14. T. Juza, Z. Sajdlova, M. Cech, V. Drastik, L. Kocvara, M. Tuser and J. Kubecka, "Improved trawling setup for sampling pelagic juvenile fish communities in small inland bodies of water," *Acta Ichthyologica et Piscatoria*, vol. 48, no. 1, pp. 105-108, 2018. <https://doi.org/10.3750/AIEP/02373>
15. S. Park and C. W. Lee, "Fuzzy control system for three-dimensional towing trajectory of trawl gear," *Ocean Engineering*, vol. 188, p. 106297, 2019. <https://doi.org/10.1016/j.oceaneng.2019.106297>
16. R. Vettor, J. Szlapczynska, R. Szlapczynski, W. Tycholiz and C. G. Soares, "Towards improving optimised ship weather routing," *Polish Maritime Research*, vol. 27, no. 01, pp. 60-69, 2020. <https://doi.org/10.2478/pomr-2020-0007>
17. S. Gucma, "Conditions of safe ship operation in seaports - optimization of port waterway parameters," *Polish Maritime Research*, vol. 26, no. 03, pp. 22-29, 2019. <https://doi.org/10.2478/pomr-2019-0042>
18. M. Wang, *Research on filter processing of trawler towing tension measurement*. Wuhan University of Technology, 2009.
19. K. I. Vinay and G. P. John, *Digital signal processing using MATLAB* (Third Edition). Science Press, 2012.
20. Z. Y. Wang, T. L. Tang, Z. Q. Xu and H. H. Ni, "Design and experiment of automatic tension control system for trawl winch on fishing boat," *Transactions of the Chinese Society of Agricultural Engineering (Transactions of the CSAE)*, vol. 33, no. 1, pp. 90-94, 2017. <https://www.tcsae.org/10.11975/j.issn.1002-6819.2017.01.012>
21. B. T. N. Nsangué, H. Tang, A. N. Pandong, L. X. Xu, D. M. Adekunle and F. X. Hu, "Examining engineering performance of midwater trawl with different horizontal spread ratio, floatage, and weight parameters: A case study of model net for Antarctic krill fisheries," *International Journal of Naval Architecture and Ocean Engineering*, vol. 14, p. 100448, 2022. <https://doi.org/10.1016/j.ijnaoe.2022.1004482092-6782>